

The 25th (2015) International Polar and Engineering Conference

Li, H., L. Lin, Z. Demirbilek, T. M. Beck, and H. R. Moritz (2015). Wave-Current Conditions and Navigation Safety at an Inlet Entrance. The 25th (2015) International Polar and engineering Conference, Kona, Big Island, Hawaii, 21-26 June, 2015, 9 pp.

Wave-Current Conditions and Navigation Safety at an Inlet Entrance

Honghai Li¹, Lihwa Lin¹, Zeki Demirbilek¹, Tanya M. Beck¹, and Hans R. Moritz²

¹US Army Engineer Research and Development Center

3909 Halls Ferry Road
Vicksburg, Mississippi, USA

²US Army Corps of Engineers, Portland District
333 SW First Ave.,
Portland, Oregon, USA

ABSTRACT

The narrow jetty configuration of Tillamook Inlet functions to constrict tidal flow, increase current speed, and prevent sediment deposition. However, the interaction of strong currents with incoming ocean waves over the inlet's ebb shoal can amplify and complicate the wave environment at the inlet entrance. In this study, the Coastal Modeling System (CMS) was used to investigate time- and space-varying wave and current conditions affecting boating operations at Tillamook Inlet and quantify the effects of physical processes. Wave simulations with refraction, shoaling, and breaking provide estimates of wave-related parameters of interest to the navigable region at Tillamook.

KEY WORDS: Navigation safety; numerical modeling; waves; current; sediment transport; channel infilling; morphology change.

INTRODUCTION

The Tillamook Inlet is located on the Pacific Northwest coast of Oregon, about 90 miles west of Portland. Five rivers drain into Tillamook Bay, a shallow estuary, which connects to the Pacific Ocean through the navigation channel that passes through a jetty-entrance and an ebb shoal, and joins with the open ocean at approximately the 80-m depth contour. The channel is well-defined from the entrance to Port of Garibaldi, the channel's termination point in Tillamook Bay (Fig. 1). The average depth in the Tillamook estuary is less than 2 m, and its dynamics is controlled by tides, wind, and surface water flows. Tillamook Bay has a mixed semi-diurnal tide with a mean tide range of 2 m and an extreme tidal range of 4.1 m (Komar 1997).

As shown in Fig. 1, the depth at the navigation channel entrance ranges between 8 m and 13 m relative to mean lower low water (MLLW), which is comparatively deeper than in the middle and backbay (estuary). There are no markers defining the channel past beyond the tips

of jetties over the ebb shoal and out in the Ocean. As such, the width and depth of the unmarked channel seaward of the entrance over the entire ebb shoal and beyond are not specified. Consequently, there is no prescribed inbound/outbound vessel route for traffic moving over the ebb shoal, where depths vary between 8 to 15 m.

Because the Tillamook Inlet is naturally self-scouring, annual surveys indicate that the dual-jettied entrance has not shoaled to the 6 m MLLW depth limit to require dredging. Both jetty heads have degraded over the years, and as of 2010, the north and south jetties had receded landward approximately 160 m and 300 m, respectively. Thus, the knowledge of local wave severity, degradation of jetties, and change in the entrance channel morphology has led the U.S. Coast Guard (USCG) to reevaluate optimal approaches to the inlet. This resulted in a new turn in the channel direction that directed vessels abruptly toward a south-oriented navigation channel (the grey polygon in Fig. 1).



Fig. 1. Location map for Tillamook Inlet and Bay, Oregon, and Port of Garibaldi. The September 2010 bathymetry with authorized navigation channel (black polygon), and the USCG preferred south channel (grey polygon).

The narrow jetty configuration functions to constrict tidal flow, increasing current speed, especially during the ebb tide. The spatial

variation of waves and currents occurring over the ebb shoal is dependent partly on the morphology of the ebb shoal that changes year to year. Because of the dynamic nature of seasonally evolving ebb shoal geometry, the resulting wave and current magnitudes over the ebb shoal and in the entrance channel can vary rapidly year around. The interaction between waves and currents in these areas can develop dangerous conditions (large steep waves and strong currents) that may pose significant risks by endangering safety and stability of vessels approaching and exiting Tillamook Inlet entrance which must pass over the ebb shoal and into the Pacific Ocean (Demirbilek et al., 2013).

The present study was conducted with the goal to identify conditions that impact navigability in Tillamook Inlet. Consequently, the primary motivation behind this study was to investigate the time- and space-varying waves and currents affecting boating operations at Tillamook Inlet for summer and winter months and to better understand the cause-effect relationship between navigability conditions at Tillamook Inlet and characteristics of the ebb- shoal, hydrodynamics of entrance, role of the jetties, and interaction between the ebb shoal, entrance and estuary.

METHOD

Coastal Modeling System

The Coastal Modeling System (CMS) was used in this investigation. As shown in Fig. 2, the CMS is an integrated suite of numerical models for waves, flows, and sediment transport and morphology change in coastal areas. This modeling system includes representation of relevant nearshore processes for practical applications of navigation channel performance, and sediment management at coastal inlets and adjacent beaches.

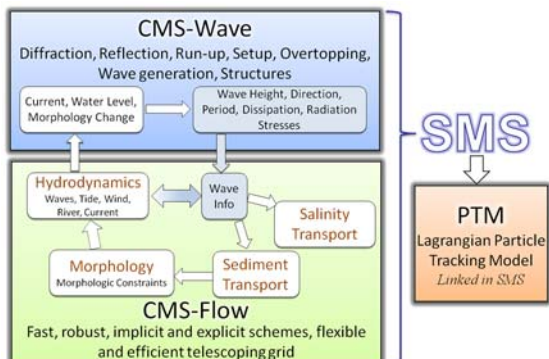


Fig. 2. The CMS framework and its components

CMS-Wave model solves the steady-state wave-action balance equation on a non-uniform Cartesian grid to simulate spectral transformation of directional random waves and is designed to simulate wave processes with ambient currents at coastal inlets and in navigation channels. The model can be used either in half-plane or full-plane mode for spectral wave transformation (Lin et al. 2011). Wind wave generation and growth, diffraction, reflection, dissipation due to bottom friction, white-capping and breaking, wave-current interaction, wave runup, wave setup, and wave transmission through structures are the main wave processes included in CMS-Wave. The height and direction of waves approaching the Tillamook Inlet navigation channel change due to wave shoaling, refraction, diffraction, reflection, and breaking. Waves propagating through the entrance interact with bathymetry, surrounding land features, currents and coastal structures. These changes to waves affect bed shear stresses and sediment mobility around this inlet.

CMS-Flow solves the conservative form of the shallow water equations that includes terms for the Coriolis force, wind stress, wave stress, bottom stress, vegetation flow drag, bottom friction, wave roller, and turbulent diffusion. Governing equations are solved using the finite volume method on a non-uniform Cartesian grid. CMS-Flow calculates hydrodynamics (water level, depth-averaged circulation), sediment transport and morphology change, and salinity due to tides, winds, waves, and river inflows (Wu et al. 2011).

The coupled CMS-Flow and CMS-Wave models were used for investigation of wave-current interaction in Tillamook Inlet. This modeling includes effects of winds, waves, tides and river inflows. The calculated quantities of interest includes wave-related engineering parameters including significant wave height (H_s , m), spectral peak period (T_p , sec) and mean wave direction ($\bar{\theta}$, deg), wave steepness (H_s / L_p , where L_p is the spectral peak wavelength calculated at the local depth), wave dissipation (m³/sec) (the wave energy loss in the wave propagation direction), and Ursell number ($H_s L_p^2 / h^3$, where h

is the local water depth) (Dally et al. 1985; Ursell 1953). Wave breaking intensity is expressed in terms of wave dissipation. Measured by significant wave height and water depth over wavelength ratio, the Ursell number helps to identify the roles of wave "nonlinearity". These engineering parameters are used to assess wave and current conditions for safe navigation, and preferred entrance and exit courses for boating operations at Tillamook Inlet.

CMS-Flow modeling task includes specification of winds, tides and river flows (discharges) to the model. The effects of waves on the circulation are input to the CMS-Flow and have been included in the simulations performed for this study. The CMS-Flow modeling considers three wave heights ($H_s = 2$ m, 3 m, and 4 m) to investigate the effects of flow on these hypothetical wave conditions. These test runs were done in part for setting up the CMS-Flow for simulations using the actual field conditions in 2005 and 2010 for the months of August (summer) and December (winter).

Wave and Flow Model Setup

Three CMS-Wave grids were generated for wave modeling: (1) an asymmetric ebb shoal grid (based on September 2005 survey), (2) a symmetric ebb shoal grid (based on June 2010 survey), and (3) a shortened South Jetty grid. All three grids cover the same square domain of 17.6 × 17.6 km with varying cell sizes from 10-m spacing. The asymmetric ebb shoal grid (Fig. 3) was generated from the September 2005 survey that shows a crescent shape ebb shoal that extends seaward from the north jetty to the inlet outer bar. The symmetric ebb shoal grid was generated from the June 2010 survey, showing a symmetric, isolated ebb shoal seaward of the inlet entrance. The shortened South Jetty grid is a hypothetical case based on the June 2010 symmetric ebb shoal grid with a truncated South Jetty recessed landward by 230 m (750 ft). This hypothetical case was simulated to evaluate whether removing a section of the South Jetty would improve navigability of the channel. The offshore boundary of the grid domain is at the 80-m isobath. Fig. 4 shows the symmetric ebb shoal grid domain and bathymetry. Fig. 5 shows the local inlet entrance bathymetry contours for the shortened South Jetty grid.

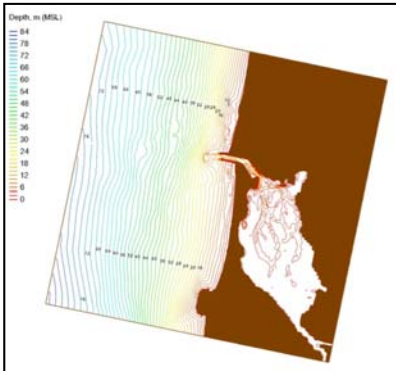


Fig. 3. CMS-Wave grid for asymmetric ebb shoal grid domain and bathymetry based on September 2005 survey, NGDC shoreline and GEODAS database.

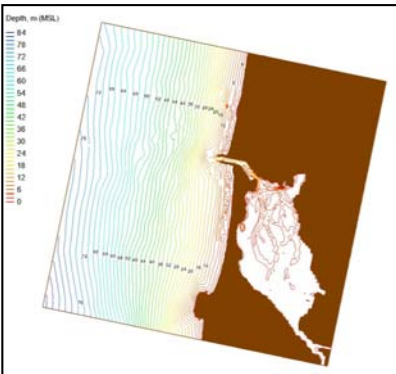


Fig. 4. Symmetric ebb shoal grid domain and bathymetry based on June 2010 survey, NGDC shoreline and GEODAS database.

A telescoping grid was used in the flow modeling that covered the same square domain as the wave grid (Fig. 6). The grid has finer resolution in areas of high interest such as the ebb shoal, entrance, inlet and Bay. The red circle denotes the location of NOAA's Garibaldi tide gage. Two red triangles denote the locations of the inlet entrance (Entrance Channel Station) and Kenchloe Point (Kenchloe Point Station) where high current were calculated. Three flow telescoping grids were generated corresponding to: (1) the asymmetric ebb shoal grid (based on September 2005 survey), (2) the symmetric ebb shoal grid (based on June 2010 survey), and (3) the shortened South Jetty grid.

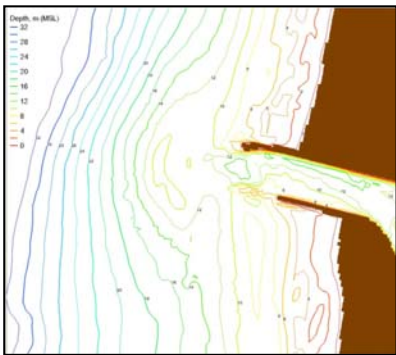


Fig. 5. Shortened south Jetty bathymetry contours.

The south jetty of the Tillamook Inlet has a recession rate of 40-80 ft/yr. Considering 15 years of the south jetty recession at a rate of 50 ft/yr, a third grid was developed using the symmetric ebb shoal bathymetry by shortening the South Jetty 230 m (750 ft). Existing and

shortened South Jetty configurations are shown in Fig. 7.

Model Forcing

Simulations were conducted for a summer (August) and a winter (December) month for asymmetric ebb shoal (September 2005 bathymetry) and symmetric ebb shoal (June 2010 bathymetry). The shortened South Jetty was simulated only for the symmetric ebb shoal. In addition to the calculation of monthly mean and maximum parameters, four peak flood and ebb current scenarios were selected to show the strong current effects on wave-related parameters. A monthly maximum estimate could be due to maximum waves or maximum currents or both. These additional scenarios ensure the peak flood and ebb current effects on wave-related parameters are included. For safety of navigation, the peak flood and ebb currents are of primary concern to boating operations.

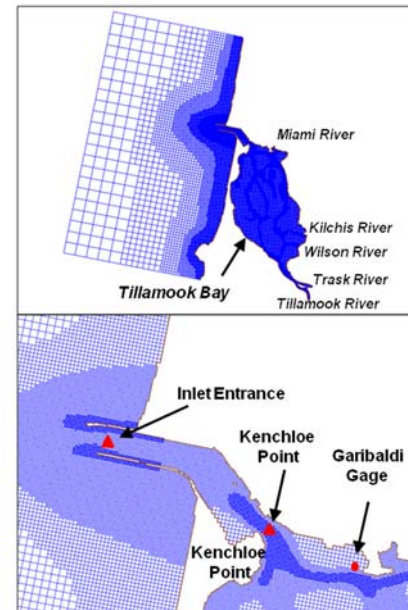


Fig. 6. CMS-Flow domain and telescoping grid.

Incident wave conditions were based on directional wave data collected by the National Data Buoy Center (NDBC, <http://www.ndbc.noaa.gov>) Buoy 46029, located approximately 60 miles northeast of Tillamook Inlet. The buoy wave data were transformed to the seaward boundary of the CMS-Wave grid using a simplified wave transformation for shore-parallel depth contours.

CMS-Flow was driven with the time-dependent water levels, winds, river discharges and waves. Water level data (see Fig. 8 for sampling data in August 2005) were obtained from NOAA coastal station (9435380) at South Beach, Yaquina River, Oregon, approximately 105 km south of Tillamook Inlet on the Oregon coast. To account for the distance between the South Beach Station and Tillamook Bay, tidal signals were phase-shifted by 30 minutes at the CMS-Flow open boundary. The data indicate no seasonal changes in tidal signals.

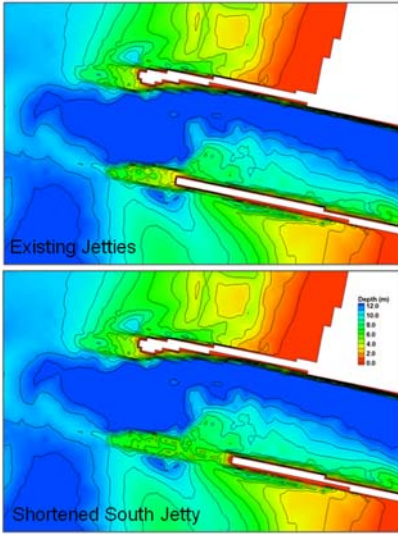


Fig. 7. Existing (top) and shortened (bottom) South Jetty configurations.

Wind data (see Fig. 9 for sampling data in August and December 2005) were obtained from the offshore NDBC Buoy 46029 as atmospheric input to flow modeling. River flow data (see Fig. 10 for sampling data in December 2010) were obtained from the USGS gages at the Trask and Wilson Rivers. The flow discharge in summer is 1 to 2 orders of magnitude smaller than the winter. The flow discharges for three other rivers (Tillamook, Kilchis, and Miami Rivers) were estimated by a weighted drainage area approach.

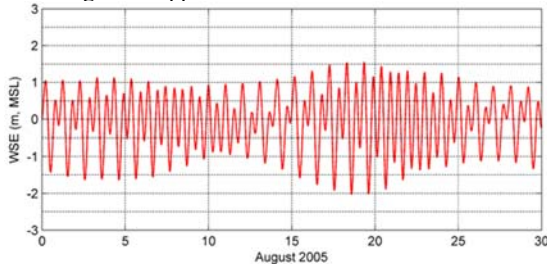


Fig 8.. Water level data for August 2005 at South Beach and Yaquina River, Oregon.

RESULTS

Simulations for Existing Jetty Condition

Water Levels and Currents

As an example, the calculated and the measured water surface elevations at Garibaldi for August 2010 are shown in Fig. 11. The calculated results show a good agreement with the measurements. Water levels at Garibaldi have a mixed signal that is mainly semi-diurnal tide. The mean tidal range (mean high water – mean low water) is 1.9 m and the maximum tidal range (mean higher high water - mean lower low water (MLLW)) is 2.5 m. Considering the size of Tillamook Bay and the narrowness of the navigation channel through Tillamook Inlet, this tidal range is large enough to generate strong ebb and flood currents at the inlet channel.

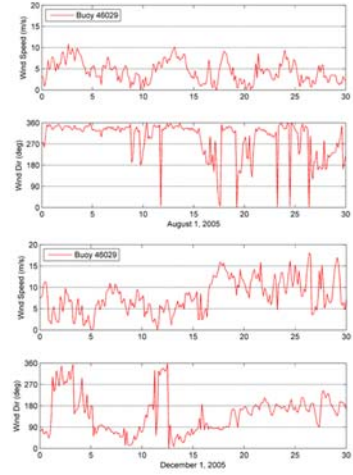


Fig. 9. Wind data for August and December 2005 at NDBC Buoy 46029.

Example snapshots of calculated current fields on 12 August 2010 at 21:00 GMT, 13 August 2010 at 03:00 GMT, 27 December 2010 at 12:00 GMT, and 18:00 GMT, are shown in Figs. 12 and 13. In these examples, incident waves are from west-northwest (300 deg azimuth) in the summer cases, and west-southwest (260 deg azimuth) in the winter cases. The calculated current magnitude reaches 3.0 m/sec at the Kenchloe Point Station (Fig. 6). The current pattern at the ebb shoal is mainly controlled by wind, waves, and local bathymetry.

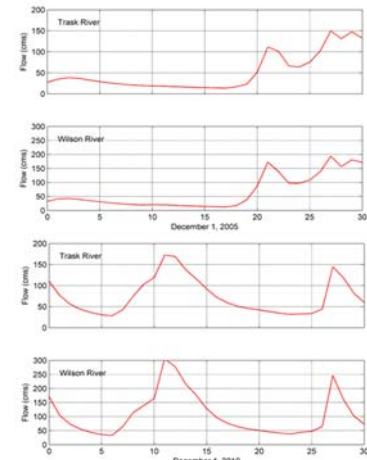


Fig. 10. River flow discharges for December 2005 and 2010 from USGS gages at Trask (#14302480) and Wilson (#14301500) Rivers, Oregon.

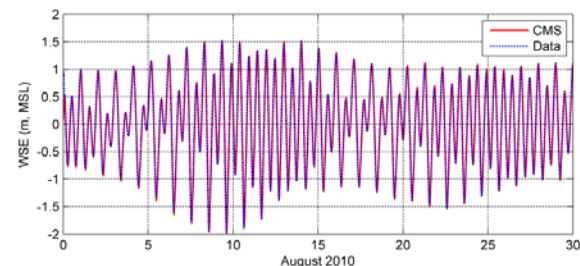


Fig. 11. Calculated water surface elevation at Garibaldi, August 2010.

Summer and Winter Monthly Simulations

Calculated monthly mean and maximum wave steepness, wave dissipation, and Ursell number for August and December 2005 are shown in Figs. 14 and 15, respectively. Monthly mean and maximum wave steepness, wave dissipation, and Ursell number for August and December 2010 are shown in Figs. 16 and 17, respectively. The values of these parameters are small in summer but larger in winter as a result of higher waves in winter. For the summer month (August), calculated mean and maximum wave steepness, dissipation and Ursell number results show that stronger wave breaking and wave nonlinearity occur over the ebb shoal in August 2005 than August 2010. Calculated maximum dissipation and Ursell numbers are relatively small in the south entrance channel. For the winter month (December), calculated mean wave steepness, dissipation and Ursell number results show stronger wave breaking and wave nonlinearity occur over the ebb shoal in December 2005 than December 2010. The values of maximum wave steepness in December 2010 are higher than December 2005. The storm waves in December 2010 have shorter mean wave periods that produce waves with larger wave steepness.

Simulations of Peak Flood and Ebb Conditions

Four scenarios of peak ebb and flood currents with large river inflows are used to show the current effects on waves. In these scenarios, the largest incident waves were around 2 m in August 2005 and 2010, and 3.4 m and 3.6 m in December 2005 and 2010, respectively. These waves came from northwest for the summer scenarios and southwest for the winter.

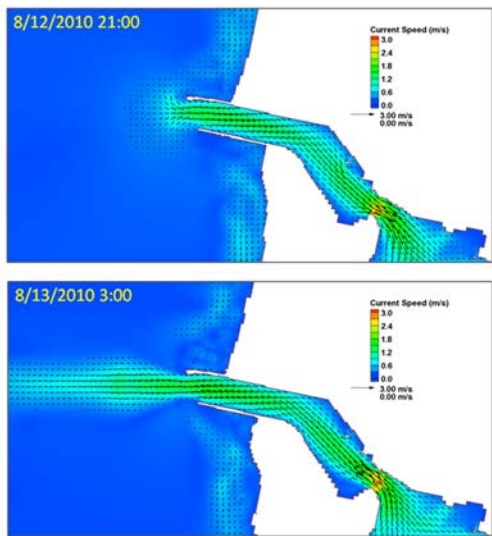


Fig. 12. Calculated current field on 12 August 2010 at 21:00 GMT (flood current) and on 13 August 2010 at 03:00 GMT (ebb current).

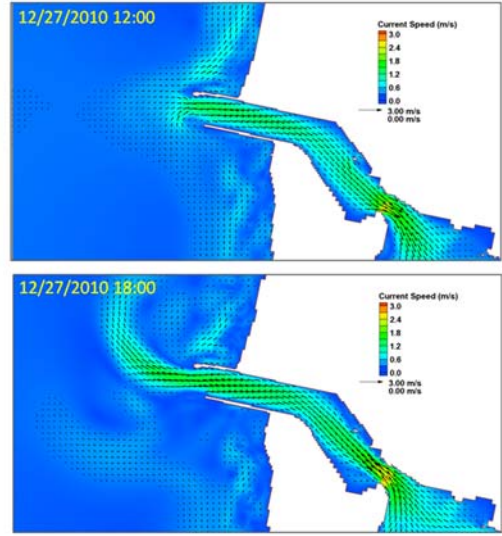


Fig. 13. Calculated current field on 27 December 2010 at 12:00 GMT (flood current) and 18:00 GMT (ebb current).

Fig. 17 shows snapshots of calculated wave steepness, wave dissipation, and Ursell number fields for a peak flood current on 12 August 2010 at 21:00 GMT and for a peak ebb current on 13 August 2010 at 03:00 GMT. These incident waves are 2.0 m (9 sec) from northwest (311 deg azimuth) and 2.1 m (9 sec) from west-northwest (294 deg azimuth), respectively. The calculated current magnitudes at the Inlet Entrance Station (Figure 5-1) are around 1.5 m/sec (see Figure 5-8). Calculated wave steepness and dissipation are higher for the peak ebb than the peak flood in the south entrance channel and ebb shoal. Calculated Ursell number fields are similar in both peak flood and ebb scenarios.

Fig. 18 shows snapshots of calculated wave steepness, wave dissipation, and Ursell number fields for peak flood and ebb currents in 27 December 2010 at 12:00 GMT and in 27 December 2010 at 18:00 GMT, respectively. The incident waves at these times were 3.4 m (11 sec) from west-southwest (259 deg azimuth) and 3.6 m (11 sec) from west-southwest (264 deg azimuth). Calculated current magnitudes at the inlet entrance were around 1.4 m/sec (see Figure 5-9). The ebb current produced larger wave steepness, dissipation, and Ursell number over the ebb shoal and south entrance channel.

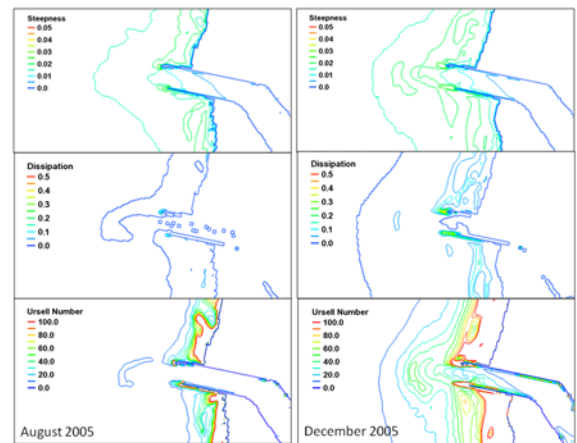


Fig. 14. Calculated monthly mean wave steepness (top), wave dissipation (middle), and Ursell number (bottom) for August and December 2005.

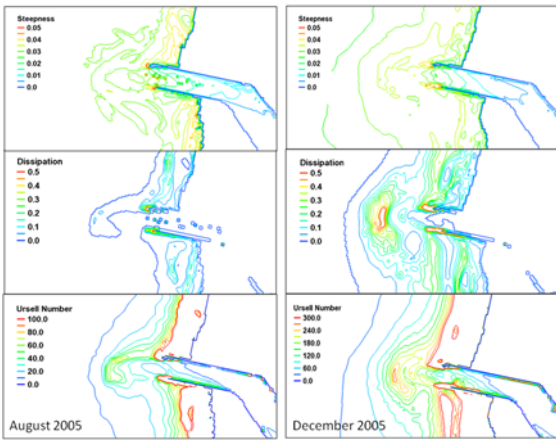


Fig. 15. Calculated maximum wave steepness (top), wave dissipation (middle), and Ursell number (bottom) for August and December 2005.

Fig. 20 shows results for one more scenario for a peak ebb current on 24 December 2010 at 03:00 GMT. The incident waves were 3.2 m and 10 sec from southwest (234 deg azimuth). The calculated ebb current magnitude at the inlet entrance was 1.7 m/sec. Compared to Figure 5-15, this scenario, with a smaller wave height and a larger current, produced smaller values of wave steepness, dissipation, and Ursell number. These results show that waves may have a stronger role than the current at the inlet entrance and ebb shoal.

Simulations for a Shortened South Jetty

Currents

For the shortened South Jetty, simulations were conducted only for August and December 2010 (symmetric ebb shoal). Fig. 21 shows calculated current fields on 12 August at 21:00 GMT and 13 August at 03:00 GMT. Fig. 22 shows the current fields on 27 December 2010 at 12:00 and 18:00 GMT. The peak flood and ebb current magnitudes at the Kenchloe Point (Fig. 5) remained unchanged between existing and shortened South Jetty simulations. With or without the South Jetty shortening, the currents at the entrance remained essentially unchanged during the ebb. The peak flood currents over the immersed section of the shortened South Jetty were reduced approximately by 0.2 m/sec (15 percent reduction) at the entrance. Results indicated that with the South Jetty shortening, the entrance becomes wider and this affects the flood current magnitude but not the ebb current magnitude.

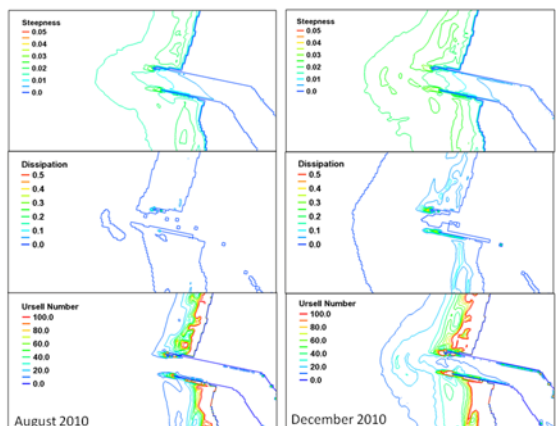


Fig. 16. Calculated monthly mean wave steepness (top), wave

dissipation (middle), and Ursell number (bottom) for August and December 2010.

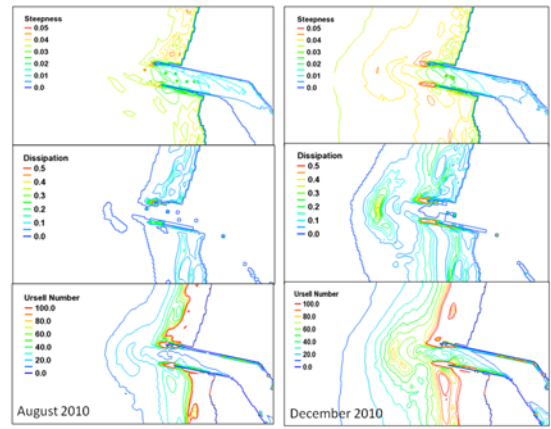


Fig. 17. Calculated maximum wave steepness (top), wave dissipation (middle), and Ursell number (bottom) for August and December 2010.

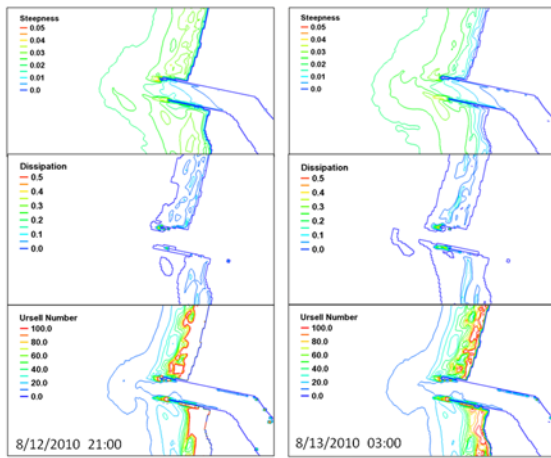


Fig. 18. Calculated wave steepness (top), wave dissipation (middle) and Ursell number (bottom) during a flood current on 12 August 2010 at 21:00 GMT and an ebb current on 13 August 2010 at 03:00 GMT.

Summer and Winter Monthly Simulations for Shortened South Jetty

Monthly mean and maximum wave steepness, wave dissipation, and Ursell number have similar patterns before and after the South Jetty shortening (Figs. 8, 9, 21, and 22). Both for summer and winter months, minor changes in wave breaking patterns occurred over the submerged section of the recessed South Jetty. Wave steepness, dissipation, and Ursell number increased and further extended into the main channel toward the Bay. This is much more noticeable for winter conditions. As we noted earlier for constant incident wave simulations, the peak values of wave steepness, dissipation, and Ursell number for the shortened South Jetty occurred approximately at the same locations of the existing (full length) South Jetty configuration.

Peak Flood and Ebb Simulations for Shortened South Jetty

Fig. 25 shows snapshots of wave steepness, wave dissipation, and Ursell number for the shortened South Jetty during a flood current on 12 August 2010 at 21:00 GMT and an ebb current on 13 August 2010 at 03:00 GMT. Fig. 26 has snapshots of wave steepness, wave dissipation, and Ursell number for the shortened South Jetty during

peak flood and ebb currents on 27 December 2010 at 12:00 GMT and on 27 December 2010 at 18:00 GMT, respectively. Comparing these to the cases of the existing jetty configuration (Figs. 10 and 11), we find that currents, wave heights, wave steepness, wave dissipation, and Ursell number have increased only over the submerged section of the shortened South Jetty. The snapshots in Fig. 18 correspond to an incident winter wave of 3.6 m from southwest, showing that waves propagate over the submerged South Jetty section to reach the navigation channel and penetrate further into the Bay.

Based on results shown in Figs. 23 through 26, the effect of South Jetty shortening was localized to the immediate vicinity of the jetty. It had little or no visible effect on waves or currents in the entrance and over the ebb shoal. For the 3-m and 5-m waves with a recessed South Jetty, there was a slight increase in wave steepness and dissipation, and waves extended a little further into the main channel. With both jetty lengths, because the full South Jetty base was modified slightly, the peak values of wave steepness and dissipation occurred at the same locations.

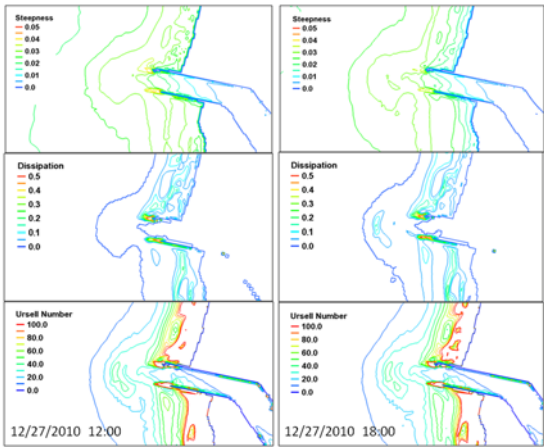


Fig. 19. Calculated wave steepness (top), wave dissipation (middle), and Ursell number (bottom) during a flood current on 27 December 2010 at 12:00 GMT and an ebb current on 27 December 2010 at 18:00 GMT.

2010 at 03:00 GMT.

CONCLUSIONS

Winds, waves, tides and river discharges were included in the combined wave and flow simulations described in this chapter. The simulations were performed with three telescoping grids corresponding to the 2005 asymmetric ebb shoal, the 2010 symmetric ebb shoal, and the 2010 shortened South Jetty. Three wave-related parameters (wave steepness, wave dissipation, and Ursell number) were calculated. The following observations are made.

The Tillamook Inlet system is affected by combined waves, tides, currents, and river discharges. Incident waves dominate the inlet and wave heights could reach 6 to 8 m during winter storms, and 3.0 m/sec peak current occur in the main channel. The current direction outside the inlet over the ebb shoal and along north and south beaches is controlled mainly by local winds, wave actions and local bathymetry. The total freshwater discharges from five rivers into Tillamook Bay can be as high as 28,000 cfs (800 m³/sec) in the winter, and these affect the ebb current.

Modeling results showed the winter storms produced larger wave steepness and wave dissipation at the inlet complex. Wave steepness and dissipation were closely associated with the bathymetry of ebb shoal, and wave dissipation patterns in the winter followed the ebb shoal shape. The calculated wave steepness and wave dissipation with the 2005 bathymetry indicated that a south passage out of the inlet would be safer than a course straight out passing over the bar or a course turning to NW direction.

Examination of the patterns produced by combined waves and flow showed that larger waves caused high wave steepness and increasing wave dissipation. The flood currents weakened wave dissipation, while ebb currents increased wave dissipation over the ebb shoal and across the USCG recommended south passage in/out of the inlet.

The shortened South Jetty reduced the flood current magnitude approximately by 0.2 m/sec (15 percent) at the entrance, but did not change the ebb flow pattern or current magnitude. The effect of South Jetty shortening was localized to the immediate vicinity of the South Jetty, and had no discernible effect on wave steepness and dissipation at the entrance and over any area of the ebb shoal. Because morphologic change that could occur over years to decades following shortening of the jetty was not considered, it is likely that the channel would migrate towards the south jetty, and therefore increasing currents over the degraded portion and potentially increasing the risks to navigation in the entrance area. Jetty shortening would also permit more wave energy to penetrate through the main channel into the Bay.

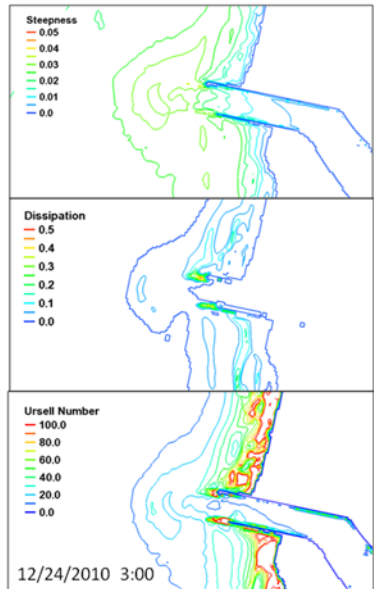


Fig. 20. Calculated wave steepness (top), wave dissipation (middle), and Ursell number (bottom) during an ebb current in 24 December

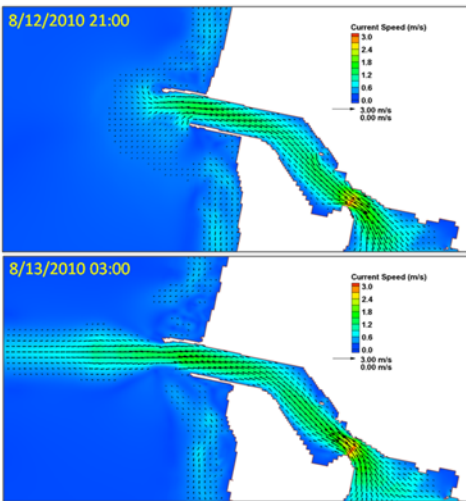


Fig. 21. Calculated current fields for the shortened South Jetty on 12 August 2010 at 21:00 GMT (flood current) and 13 August 2010 at 03:00 GMT (ebb current).

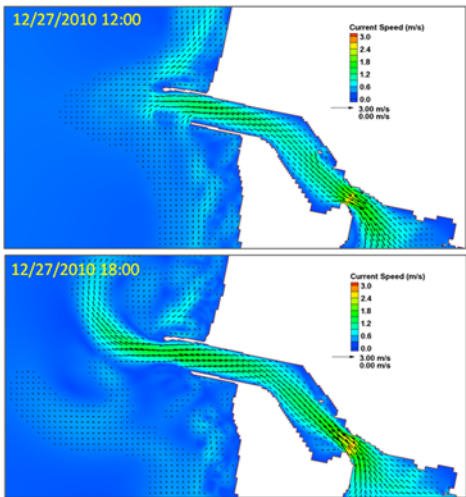


Fig. 22. Calculated current fields for the shortened South Jetty on 27 December 2010 at 12:00 GMT (flood current) and 18:00 GMT (ebb current).

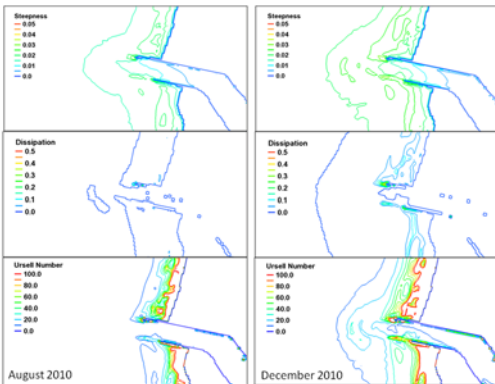


Fig. 23. Monthly mean wave steepness (top), wave dissipation (middle), and Ursell number (bottom) fields for the shortened South Jetty in August and December 2010.

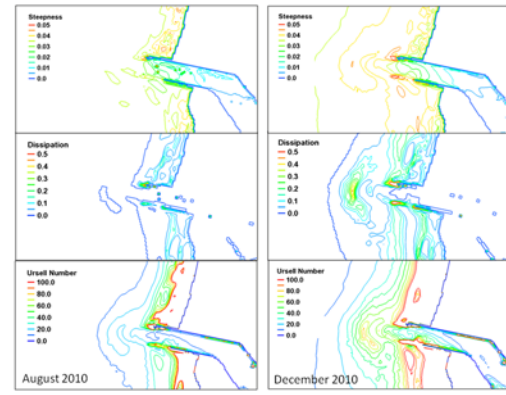


Fig. 24. Maximum wave steepness (top), wave dissipation (middle), and Ursell number (bottom) fields for the shortened South Jetty in August and December 2010.

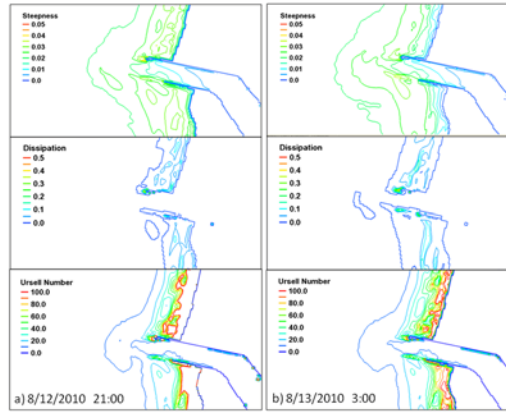


Fig. 25. Wave steepness (top), wave dissipation (middle), and Ursell number (bottom) for the shortened South Jetty: a) flood current in 12 August 2010 at 21:00 GMT and b) ebb current in 13 August 2010 at 03:00 GMT.

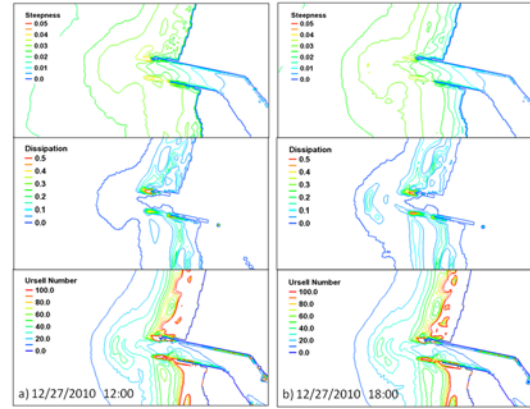


Fig. 26. Wave steepness (top), wave dissipation (middle), and Ursell number (bottom) for the shortened South Jetty: a) flood current on 27 December 2010 at 12:00 GMT and b) ebb current on 27 December 2010 at 18:00 GMT.

ACKNOWLEDGEMENTS

Permission was granted by the Chief, U. S. Army Corps of Engineers to publish this information.

REFERENCES

Dally, W. R., Dean, R. G., Dalrymple, R. A. (1985). Wave height variation across beaches of arbitrary profile. *Journal of Geophysical Research*, 90 (C6): 11917-11927.

Demirbilek, Z., Li, H., Lin, L., Beck, T. M., and Moritz, H. R. (2013). "Preliminary Analysis of Morphology Change, Waves, and Currents for Navigation at Tillamook Inlet, Oregon," ERDC/CHL-TR-13-13, US Army Engineer Research and Development Center, Coastal and Hydraulics Laboratory, Vicksburg, Mississippi.

Komar, P. D. (1997). Sediment Accumulation in Tillamook Bay, Oregon, A Large Drowned-River Estuary. Report for the Tillamook Bay National Estuary Project, Oregon.

Lin, L., Demirbilek, Z., and Mase, H. (2011). Recent capabilities of CMS-Wave: A coastal wave model for inlets and navigation projects. *Proceedings, Symposium to Honor Dr. Nicholas Kraus, Journal of Coastal Research, Special Issue 59*, 7-14.

Ursell, F. (1953). The long-wave paradox in the theory of gravity waves. *Proceedings of the Cambridge Philosophical Society* 49 (4): 685-694.

Wu, W., Sanchez, A., and Zhang, M. (2011). An Implicit 2-D Shallow Water Flow Model on Unstructured Quadtree Rectangular Mesh. *Proceedings, Symposium to Honor Dr. Nicholas Kraus, Journal of Coastal Research, Special Issue 59*, 15-26.